

# Spatial reconstruction of Scottish summer temperatures from tree rings

Miloš Rydval,<sup>a,b,\*</sup> Björn E. Gunnarson,<sup>c</sup> Neil J. Loader,<sup>d</sup> Edward R. Cook,<sup>e</sup> Daniel L. Druckenbrod<sup>f</sup> and Rob Wilson<sup>a,e</sup>

<sup>a</sup> School of Geography and Geosciences, University of St Andrews, UK

<sup>b</sup> Faculty of Forestry and Wood Sciences, Czech University of Life Sciences Prague, Czech Republic

<sup>c</sup> Department of Physical Geography and Quaternary Geology, Stockholm University, Sweden

<sup>d</sup> Department of Geography, Swansea University, UK

<sup>e</sup> Lamont-Doherty Earth Observatory, Columbia University, Palisades, NY, USA

<sup>f</sup> Department of Geological, Environmental, and Marine Sciences, Rider University, Lawrenceville, NJ, USA

**ABSTRACT:** A detailed understanding of past temporal patterns and spatial expression of temperature variations is important to place recent anthropogenic climate change into a longer term context. In order to fill the current gap in our understanding of northwest European temperature variability, point-by-point principal component regression was used to reconstruct a spatial field of 0.5° temperature grids across Scotland. A sequence of reconstructions utilizing several combinations of detrending and disturbance correction procedures, and a selection of tree-ring parameters [including ring width (RW), maximum latewood density (MXD) and blue intensity (BI)] was used in an evaluation of reconstruction skill. The high resolution of the reconstructed field serves also as a diagnostic tool to spatially assess the temperature reconstruction potential of local chronologies. Best reconstruction results, reaching calibration  $r^2 = 65.8\%$  and verification  $r^2 = 63.7\%$  in central Scotland over the 1901–1976 period, were achieved using disturbance-corrected and signal-free detrended RW chronologies merged with BI data after low-pass (high-pass) filtering the RW (BI) chronologies. Calibration and verification  $r^2 > 50\%$  was attained for central, north and east Scotland,  $>40\%$  in west and northwest, and  $>30\%$  in southern Scotland with verification of nearly all grids showing some reconstruction skill. However, the full calibration potential of reconstructions outside central Scotland was reduced either due to residual disturbance trends undetected by the disturbance correction procedure or due to other climatic or non-climatic factors which may have adversely affected the strength of the climate signal.

**KEY WORDS** dendroclimatology; tree ring; temperature; spatial reconstruction; Scots pine; Scotland

Received 20 December 2015; Revised 28 April 2016; Accepted 12 May 2016

## 1. Introduction

Anthropogenically induced climate change presents a monumental challenge for the international community (IPCC, 2014). To provide a context for recent climatic trends and their link to anthropogenic activity, it is essential to continue improving our understanding of ‘natural’ climatic variability and mean state changes in the past. Considering the temporal and spatial limitations of the available network of instrumental measurement stations, which provide direct records of past temperature variability, palaeoclimatic proxy archives in general, and in particular annually resolved and absolutely dated tree-ring records, represent a valuable resource for extending and improving our understanding of climatic behaviour in the past. Data from tree rings can additionally offer valuable information about climatic and environmental conditions in locations for which no instrumental records exist.

While large-scale hemispheric reconstructions of climatic variability have received considerable attention, the importance of moving the focus towards the development of finer scale, denser networks of regional reconstructions has been highlighted (e.g. Wilson and Luckman, 2003; Jones *et al.*, 2009; Ahmed *et al.*, 2013). By increasing the spatial resolution of reconstructions, a more accurate understanding of local and regional-scale climatic variability can be achieved if actual regional variations are captured.

A range of techniques have been developed to investigate large-scale spatial patterns of recent and pre-instrumental climatic variability. Researchers have in the past utilized a range of methods for the development of spatial climate reconstructions, including for example regularized expectation maximization (RegEM – Schneider, 2001; Zhang *et al.*, 2004), canonical regression/canonical correlation analysis (CCA – Fritts, 1976; Barnett and Preisendorfer, 1987) and orthogonal spatial regression (OSR – Briffa *et al.*, 1986; Cook *et al.*, 1994).

The point-by-point regression (PPR – Cook *et al.*, 1999) method is used here to reconstruct summer temperature

\* Correspondence to: M. Rydval, School of Geography and Geosciences, Irvine Building, University of St Andrew, North Street, St Andrews, KY16 9AL, Fife, Scotland, UK. E-mail: rydval@gmail.com; mr268@st-andrews.ac.uk

grids covering Scotland. PPR utilizes principal component regression (PCR) to reduce a network of site chronologies to the dominant modes of variance, and these PC scores are used for the regression-based reconstruction of the target predictand. PPR is a nuance over OSR methods as it only utilizes sites for a particular location within a specified distance. Therefore, one important characteristic of PPR is that it utilizes 'local' chronologies proximal to the reconstructed grids and, unlike some approaches, does not rely on large-scale teleconnections (Dannenber and Wise, 2013). The PPR method was initially developed and applied by Cook *et al.* (1999) to reconstruct nearly 300 years of drought over the conterminous United States as expressed by gridded Palmer Drought Severity Index (PDSI) data. This work was expanded to investigate up to 1200 years of drought history in the western United States (Cook *et al.*, 2004). More recently, the approach was also applied outside North America to reconstruct spatial patterns of monsoon variability and drought in Asia (Cook *et al.*, 2010) and Europe (Cook *et al.*, 2015). Using the same method, a hydroclimatic reconstruction was also performed by Seftigen *et al.* (2014) for Fennoscandia, and Fang *et al.* (2011) applied the approach to reconstruct precipitation patterns in China. A spatial reconstruction of drought was also developed by Touchan *et al.* (2011) for northwest Africa, and Cook *et al.* (2016) performed a spatiotemporal analysis of drought in the Mediterranean based on the Cook *et al.* (2015) reconstruction.

Despite its origins and predominant application in the context of hydroclimate (and drought) reconstruction, the utilization of PPR to reconstruct temperature, although more limited, has also been successfully undertaken. For example, the method has been used to reconstruct temperature for China (Shi *et al.*, 2012) and the broader East Asian region (Cook *et al.*, 2013). A modified version of PPR has also been used to develop a 500-year multi-proxy temperature reconstruction for China (Yang *et al.*, 2013). Utilization of the PPR approach for the reconstruction of European climate has so far been limited, and although Luterbacher *et al.* (2004) used OSR to perform a climate field reconstruction of European temperature, the work described in this study is the first instance of a PPR-based spatial reconstruction of temperature in Europe.

Herein, a series of experiments are presented in which summer temperature grids are reconstructed as a spatial field spanning 54.5°–59°N and 1.5°–7.5°W representing Scotland (Figure 1). Rather than primarily focusing on the methodological subtleties of the PPR process itself, which have already been extensively investigated (e.g. Cook *et al.*, 1999, 2013), this study focuses on differences in reconstruction characteristics as a result of selecting particular sets of tree-ring parameters and applying various methods for the development of tree-ring chronologies (including standardization and non-climatic disturbance trend removal). In addition, this work applies the method on a smaller scale than has typically been performed in the past by reconstructing a field with a 0.5°-by-0.5° grid resolution, which is appropriate considering the relatively small size of the investigated region. The purpose of this

research is therefore not merely to attempt the development of a robust spatial temperature reconstruction, but also to develop an understanding of the strengths and weaknesses of the current Scottish tree-ring network used to develop the reconstructions. The subsequent implications of differences in the strength and robustness of individual grid reconstructions allows PPR to be applied here as a diagnostic tool, indicating where chronology improvement is required in the future.

## 2. Methods

### 2.1. Study area

Scotland experienced a protracted period of deforestation, reaching an all-time high in the first half of the 19th century followed by reforestation efforts in the 20th century and particularly after the Second World War (Mather, 2004). Total forest cover in Scotland likely reached a minimum of ~5% between the 17th and early 20th century (Mather, 2004; Smout *et al.*, 2005), and increased to 17.8% by 2010 (Forestry Commission, 2011), although only ~1% of semi-natural forest cover remains in Scotland at present (Crone and Mills, 2002). The current forests mostly consist of residual semi-natural pine stands and represent the NW limit of the range of Scots pine in Eurasia (Kinloch *et al.*, 1986).

Scotland is characterized by a temperate oceanic climate (Gallardo *et al.*, 2013). The strong influence of the Gulf Stream moderates and contributes to the mild climate conditions (Dawson, 2009). Mean annual temperatures generally remain around 9–10 °C in lowland areas of the mainland but decrease in the north and with increasing elevation, with lowest mean temperatures of ~1 °C in high elevations in the Cairngorm Mountains of central Scotland (Met Office, 2015). Summer temperatures in Scotland are among the coolest in Europe. Precipitation is primarily controlled by distance from the Atlantic Ocean and topography/orography with most precipitation concentrated in parts of the west and northwest of the country, decreasing towards the east and southeast. Mean annual precipitation reaches 4000 mm in parts of the west Highlands with lows of <700 mm in parts of the east coast (Steven and Carlisle, 1959; Met Office, 2015). There is a steep precipitation gradient from west to east with amounts in parts of west and northwest among the highest in Europe, while precipitation in the east of Scotland is more typical for the European continent. Wind is an important limiting factor which restricts the northern limit of pine in Scotland and also acts to lower the treeline elevation (Körner, 1998; Moir, 2008) due to high-wind stress in the west and northwest of the country (Quine and White, 1993).

NW Europe is particularly sensitive to the influences of synoptic scale atmospheric and oceanic phenomena and climatic modes of variability such as the North Atlantic Oscillation (NAO – Hurrell, 1995; Hurrell and van Loon, 1997), the Arctic Oscillation (Thompson and Wallace, 1998) and the Atlantic Multidecadal Oscillation (Schlesinger and Ramankutty, 1994). Climate in Scotland

SPATIAL RECONSTRUCTION OF SCOTTISH SUMMER TEMPERATURES

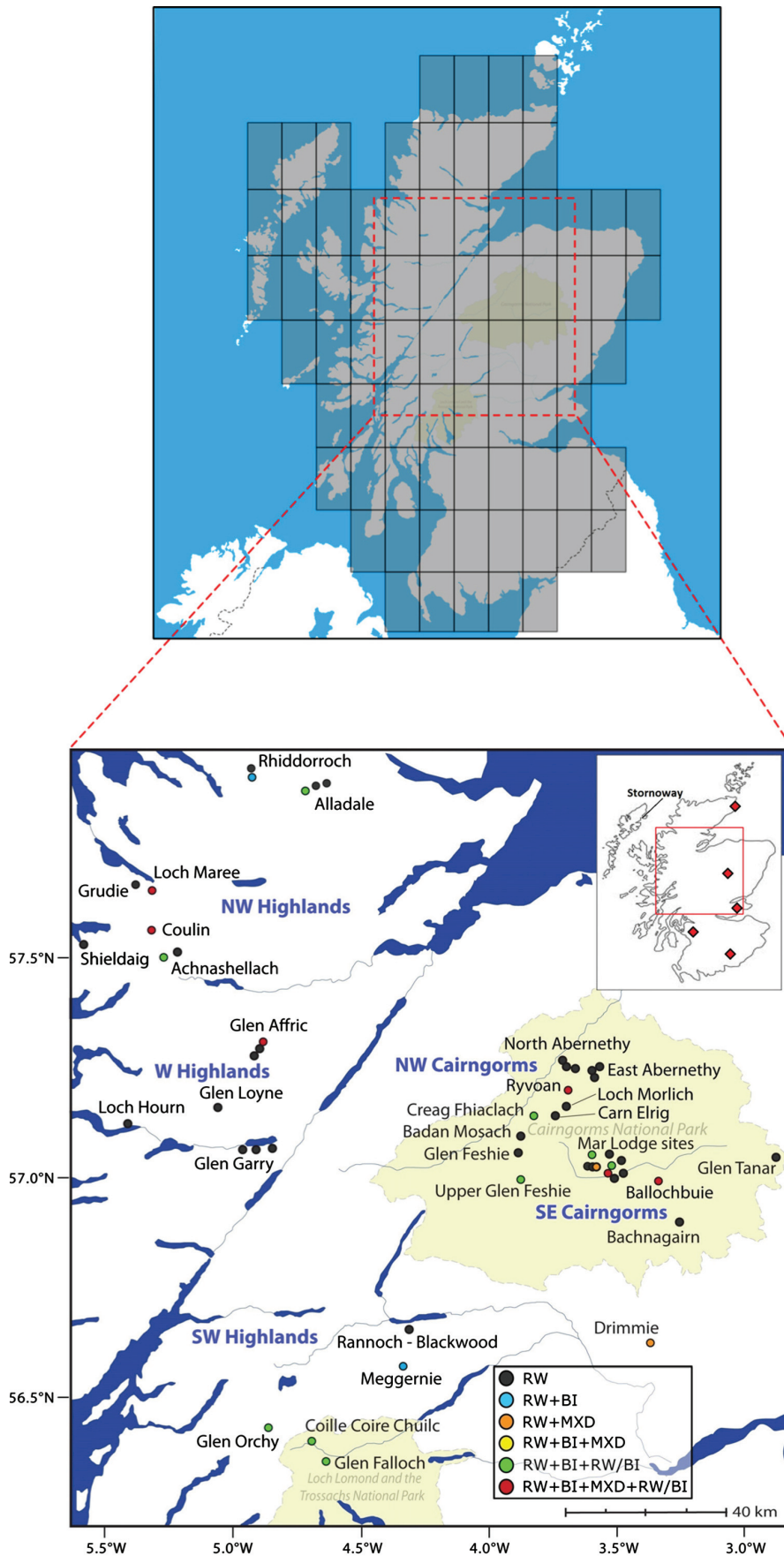


Figure 1. Map of Scotland and location of field containing 76 individual 0.5° reconstruction grids along with the location of RW, BI, MXD and composite BI/RW site chronologies used for spatial reconstruction (approximate locations of instrumental records included in the SMT temperature series are marked in the inset map).

is strongly affected by weather patterns associated with the influence of North Atlantic climate. The NAO is a dominant pattern of atmospheric circulation in the North Atlantic and an important determinant of weather and climate in Scotland and other parts of Europe with the strongest influence in winter months (Hurrell *et al.*, 2003; Hurrell and Deser, 2010). In Scotland, a positive phase of the NAO typically leads to increased precipitation, milder temperatures and increased wind-storm occurrence and severity, whereas a negative phase leads to more common incidence of seasonal temperature extremes (e.g. colder winter conditions) and reduced precipitation (Trigo *et al.*, 2002; Hurrell and Deser, 2010). Tree-ring chronologies from Scotland are ideally suited (due to their location and seasonal response) to reconstruct the summer counterpart of the NAO (SNAO), whose southern node is centred on Scotland (Folland *et al.*, 2009; Linderholm *et al.*, 2009).

## 2.2. Tree-ring network and chronologies

Based on a network of 44 ‘living’ Scots pine sites around Scotland (Figure 1), 40 ring width (RW), 16 blue intensity (BI) and 8 maximum latewood density (MXD) chronologies were used to develop a spatial temperature reconstruction for Scotland (see Table 1). Chronologies from four sites in the northwest Cairngorms were excluded from analysis and retained for the development of an independent temperature reconstruction extended with subfossil samples from the same area as part of a separate study (Rydval, 2015). In addition, 14 chronologies consisting of composite [combined high frequency (high-pass) BI and low frequency (low-pass) RW data] from 14 of the sites were also used for the reconstruction of the temperature field. RW and MXD chronologies were supplemented with data from seven sites previously used in the Hughes *et al.* (1984) Edinburgh summer temperature reconstruction, and which are available from the International Tree-Ring Data Bank (ITRDB, 2014).

## 2.3. RW chronology development

Measurement of samples was performed according to established dendrochronological practices (Stokes and Smiley, 1968) with either Coorecorder using scanned images (Larsson, 2014) or a Velmex traversing measuring stage (directly from sample) to a precision of 0.001 mm. CDendro (Larsson, 2014) and COFECHA (Holmes, 1983) were used to verify series crossdating. RW chronologies were developed by detrending measurement series using negative exponential or linear functions (NX) in ARSTAN (Cook and Holmes, 1986) or NX with signal-free standardization (SF) (Melvin and Briffa, 2008).

The impact of disturbance related to human activity on forest ecosystems is not uncommon and has been reported for example in Scandinavia even in areas considered undisturbed (Josefsson *et al.*, 2010) and has been shown to affect the climate signal in RW chronologies from such locations (Gunnarson *et al.*, 2012). Rydval *et al.* (2016) identified the presence (and succeeded in reducing the

influence) of disturbance-related growth release trends in several Scots pine RW chronologies which were attributed to a history of extensive woodland timber extraction over several centuries in Scotland. As the presence of disturbance trends in RW chronologies can obscure decadal and longer term trends related to climatic variability, use of these ‘disturbance-corrected’ chronologies in temperature reconstructions is explored here.

The potential presence of disturbance trends (hypothesized to be primarily related to timber extraction and clearance) in some chronologies of the Scottish tree-ring network was assessed in Rydval *et al.* (2016) using the curve intervention detection (CID) method. This time-series-based intervention detection technique, based on methods presented in Druckenbrod (2005) and Druckenbrod *et al.* (2013), objectively detects disturbance trends in individual RW series. As part of the disturbance detection procedure, a constant of 1 mm is added to all series measurements to enable effective detection and correction without the loss of information. In the procedure, individual series are power transformed (Cook and Peters, 1997) and detrended using negative exponential or linear function. For each series, disturbance trends are identified as outliers from a distribution of running means (with window lengths from 9 to 30 years) based on a residual time-series of AR model estimates and the detrended RW series (Druckenbrod *et al.*, 2013). From this distribution, outliers are classified when a running mean value exceeds a scale of 3.29 from the bi-weight mean (Mosteller and Tukey, 1977) of the distribution. The disturbance trend is then removed by fitting a curve (Warren, 1980) to the RW series at the point where the disturbance-related growth release is identified. The procedure is performed iteratively for each series until no further outliers are identified.

This time-series-based intervention detection method was shown to successfully reduce the influence of disturbance in the majority of Scottish chronologies affected by disturbance. A detailed description of this method and its application to the Scottish RW chronologies used in this study is presented in Rydval *et al.* (2016). In that study, an assessment of whether the before correction (pre-CID) or after correction (post-CID) versions of SF chronologies should be utilized to reconstruct summer temperature was performed using correlation analysis to compare the RW chronologies with instrumental temperature data and a Scotland-wide MXD chronology composite. The selection of chronology versions to be used here for temperature reconstruction was based on that assessment and the results of this selection process are summarized in Table 1. A summary of pre- and post-CID chronologies, representing three regional groupings, and a comparison with instrumental temperature data is presented as Figure S1, Supporting Information.

## 2.4. BI and MXD chronology development

The process for the development of BI chronologies and the set of procedures associated with it have evolved over time (i.e. sample treatment and measurement techniques

Table 1. Summary of site elevation, RW chronology versions (pre- or post-CID correction) used for temperature reconstruction and RW, BI, composite RW/BI and MXD chronology range used for reconstruction after truncation – EPS  $\geq$  0.7 and minimum number of RW, BI series  $\geq$  8 and MXD series  $\geq$  5.

Site name	Site code	Site elevation (m a.s.l.)	RW version used	RW range	BI range	Composite RW/BI range	MXD range
Abernethy – east	ABE	340–450	Post-CID	1749–2009	–	–	–
Abernethy – north	ABN	240–340	Post-CID	1863–2009	–	–	–
Achnashellach East/West <sup>a</sup>	ACEW	100–130	Pre-CID/post-CID	1742–2009	– <sup>b</sup>	1872–2008 <sup>c</sup>	–
Alladale	ALD	280–380	Post-CID	1731–2012	1768–2011	1737–2012	–
Bachnagairn	BAG	500–560	Post-CID	1838–2008	–	–	–
Ballochbuie	BAL	300–500	Pre-CID	1663–2011	1736–2010	1733–2010	1727–2010
Badan Mosach	BAM	370–420	Post-CID	1840–2008	– <sup>b</sup>	–	–
Coille Choire Chuilc	CCC	210–280	Post-CID	1825–2011	1825–2011	1830–2010	–
Coulin	COU	250	Post-CID	1697–2009	1763–2008	1764–2008	1765–1978
Creag Fhiaclach	CRF	500–550	Post-CID	1756–2009	1792–2008	1792–2008	–
Carn Elrig	CRNE	480–540	Pre-CID	1821–2008	–	–	–
Drimmie	DRIM	215	Pre-CID	1831–2010	–	–	1837–1976
Glen Affric	GAF	300	Post-CID	1712–2013	1763–2012	1747–2012	1769–2012
Glen Derry East	GDE	480–530	Pre-CID	1742–2008	–	–	1784–1978
Glen Derry North	GDN	530–600	Pre-CID	1604–2010	1621–2009	1621–2009	–
Glen Derry West	GDW	450–520	Pre-CID	1768–2008	–	–	–
Glen Feshie	GF	480–540	Pre-CID	1847–2006	–	–	–
Ghleann East	GLE	490–540	Pre-CID	1749–2008	–	–	–
Glen Falloch	GLF	160–200	Pre-CID	1595–2011	1628–2010	1624–2010	–
Glen Garry	GLG	190	Pre-CID	1793–2009	–	–	–
Ghleann West	GLW	480–550	Pre-CID	1760–2008	–	–	–
Glen Orchy South	GOS	200–210	Post-CID	1829–2009	1845–2008	1864–2008	–
Grudie	GRD	70–120	Post-CID	1716–2009	–	–	–
Glen Tanar	GTA	306–379	Pre-CID	1803–2012	–	–	–
Loch Hourn	HOU	90–240	Post-CID	1853–2007	–	–	–
Inverey	INV	500–550	Pre-CID	1730–2011	1725–2010	1733–2010	1735–1976
Loch Maree	LM	100	Post-CID	1745–2009	1824–2008	– <sup>d</sup>	1808–1978
Glen Loyne	LOY	240–370	Post-CID	1542–2007	–	–	–
Luibeg	LUI	460–540	Pre-CID	1702–2008	–	–	–
Meggernie	MEG	325	Pre-CID	1848–2011	1848–2010	– <sup>d</sup>	–
Mar Lodge	ML	350	Pre-CID	1835–2008	– <sup>b</sup>	–	–
Loch Morlich	MOR	410–450	Pre-CID	1775–2009	–	–	–
Punch Bowl	PNB	450–550	Post-CID	1837–2008	–	–	–
Quoich	QUO	430–500	Pre-CID	1704–2011	1765–2010	1764–2010	–
Rannoch	RANN	320	Post-CID	1788–2010	–	–	–
Rhiddoroch	RHD	180–230	Pre-CID	1760–2012	1766–2011	– <sup>d</sup>	–
Ryvoan	RYO	420–480	Pre-CID	1790–2011	1797–2010	1792–2010	1800–2010
Shieldaig	SHG	10–100	Pre-CID	1860–2011	– <sup>b</sup>	–	–
Upper Glen Feshie	UGF	400–520	Pre-CID	1761–2010	1758–2009	1761–2009	–

<sup>a</sup>For this study, both Achnashellach sites were composited together to improve replication. <sup>b</sup>BI chronology is not used due to poor signal strength and/or insufficient chronology length. <sup>c</sup>Signal strength sufficiently strong to include BI high frequency in composite RW/BI chronology. <sup>d</sup>Composite RW/BI chronology not developed due to poor coherence of RW low frequency with climate.

have changed and developed). Wilson *et al.* (2012) noted that limitations in the low frequency component existed in some of the earlier generated Scottish BI chronologies because of inadequate resin extraction and this observation was supported by a more detailed examination of BI in Rydval *et al.* (2014). Consequently, the expression of low frequency trends in these data may be limited and express non-climatic trends related to colour differences between the heartwood and sapwood.

Although older MXD series data (Hughes *et al.*, 1984) were obtained from the ITRDB tree-ring archive, the remaining (more recently developed) MXD and BI chronologies were developed following the procedures described in Rydval *et al.* (2014). An ITRAX multiscanner from Cox Analytical Systems was used to generate the

newer MXD data following standard sample preparation techniques (Schweingruber *et al.*, 1978). A twin-bladed circular saw was used to cut 1.2 mm thick laths followed by 24 h resin extraction treatment with ethanol in a Soxhlet apparatus. After air drying to 12% water content, the laths were X-rayed in the ITRAX system to produce 1270 dpi inverted grey scale images subsequently calibrated using a 1.274 g cm<sup>-3</sup> cellulose acetate calibration wedge from Walesch Electronic (Schweingruber, 1988). The density data were measured from the images using WinDendro (Guay *et al.*, 1992). For two sites (Ballochbuie and Glen Affric) for which both archived and newly developed MXD data exist, the older and newer subsets were combined as no significant differences were identified between the subsets.

For BI measurement, samples were immersed in acetone for a 72-h period to extract resins and sanded after drying up to 1200 grit grade. The samples were scanned with a Canon CanoScan 9000 F flatbed scanner along with SilverFast Ai (v.8.0.1.24) software. A Kodak IT8.7/2 calibration target was used with the SilverFast IT8 calibration procedure to calibrate the scanner and samples scanned with 2400 dpi resolution. A box with a non-reflective inner surface was used while scanning to avoid ambient light biases. BI was measured with Coorecorder software (Larsson, 2014) and BI series were then inverted. For the purposes of this study, detrending of MXD and BI series (after inversion) was performed by fitting negatively sloping (or zero slope) linear functions. Index calculation was carried out by subtraction in ARSTAN and stabilization of chronology variance was performed (Osborn *et al.*, 1997).

All chronologies used for further analysis were truncated to periods with EPS  $\geq 0.7$  and replication  $\geq 8$  series for BI and RW (Table 1). The same EPS limit and replication of  $\geq 5$  series was used as the cut-off for MXD data. Although an EPS threshold of 0.85 is commonly used, a lower limit of 0.7 was adopted to maximize the useable chronology span and due to the fact that the common regional signal is effectively increased as a result of the utilization of PCR rather than utilizing chronologies individually.

### 2.5. Composite high-pass BI/low-pass RW chronology development

Previous research by Guiot (1985) demonstrated potential advantages of applying digital filtering techniques to perform a climate reconstruction by decomposing a predictor and predictand into separate frequency bands using mutually exclusive filters. This technique was further explored by Osborn and Briffa (2000) who investigated timescale-dependence in the context of temperature reconstruction development by performing regression separately on several frequency bands of decomposed predictor/predictand time-series, noting that this can lead to improved estimation of past temperature. The approach of Guiot (1985) was also successfully applied by Guiot (2012) to perform a multi-proxy reconstruction of April to September European temperature. Herein, however, a variation on the approach applied in Briffa *et al.* (2013) is explored by combining separate frequency bands from chronologies of two parameters. This procedure was performed in an attempt to exploit some of the advantages of BI (i.e. stronger high frequency response to temperature than RW – Rydval *et al.*, 2014) and RW chronologies (i.e. stronger expression of low frequency trends and not biased by colour changes in the wood) after undertaking non-climatic disturbance trend removal (Rydval *et al.*, 2016).

For each site where sufficiently long and well-replicated BI and RW chronologies were available (based on criteria discussed above), new composite time-series were developed by combining high to intermediate frequency bands of BI chronologies with low to intermediate frequency bands of RW chronologies using the programme AnClim

(Štěpánek, 2008). Although the optimal seasonal response of the two tree-ring parameters differed for some site chronologies, in such cases, a compromise was reached to find a common climatic season in order to assess coherency at a range of frequencies between the tree-ring and instrumental temperature data of the respective  $0.5^\circ$  grid. For this purpose, coherence analysis was applied to predictor (BI/RW) and predictand (mean seasonal temperature) data to determine a common frequency cut-off. This cut-off was identified for each pair of site chronologies as the intersection of decreasing coherence between BI and instrumental data from higher to lower frequencies and decreasing coherence between RW and instrumental data from lower to higher frequencies (see Figure S2 for an example). The RW (BI) chronologies were then low-pass (high-pass) filtered using a Gaussian filter with the identified frequency cut-off. The  $0.5^\circ$  grid seasonal instrumental temperature series were also filtered to produce low-pass and high-pass filtered versions using the same cut-off for the common season identified for each respective pair of RW/BI chronologies. The low-pass (high-pass) filtered RW (BI) series were then scaled (same mean and standard deviation; Esper *et al.*, 2005) to their corresponding low-pass (high-pass) filtered seasonal temperature series and the low-pass RW and high-pass BI components subsequently added together to form a single composite BI/RW chronology.

### 2.6. Reconstruction procedure

The PPR method was used here to reconstruct spatial patterns of past temperature variability within a grid consisting of 76 individual  $0.5^\circ$  CRU TS3.10 mean temperature boxes (Figure 1; Harris *et al.*, 2014). Additional reconstruction assessments were also performed using Scottish mainland temperature (SMT) data published by Jones and Lister (2004), which are composed of five instrumental records from mainland stations (Auchincruive/Paisley, Braemar, Eskdalemuir/Dumfries, Leuchars/Edinburgh and Wick – see inset map in Figure 1 for approximate record locations. Note that the Auchincruive, Eskdalemuir and Leuchars series were extended with the Paisley, Dumfries and Edinburgh series, respectively – see Jones and Lister (2004) for details). Although some variability regarding the optimal season for the range of site and parameter chronologies was identified, overall, July–August (JA) was found to be the predominant consistent optimal season for BI, MXD and composite (high-pass BI/low-pass RW) chronologies. A good response to JA temperatures was also evident in the RW data. The JA season was therefore selected as the compromise reconstruction target. This selection was also partly motivated as Hughes *et al.* (1984) reconstructed this season.

For the PPR procedure, an initial search radius of 35 km was used to identify chronologies within or in close proximity to each reconstructed grid. If within this search radius a suitable number of chronologies could not be found, the radius was expanded by an additional 50 km. By restricting the search radius in this way and including

only proximal chronologies, a more spatially explicit spatial reconstruction can be achieved.

Prior to principal component analysis, chronologies were screened using correlation with the instrumental data (one-tailed  $p < 0.10$ ) to exclude weak chronologies. Only tree-ring data for the 'current year' ( $t=0$ ) were used as predictor variables. Lagged predictors (i.e. from previous or subsequent years relative to the reconstructed year) were not considered in the analysis as no significant influence of previous year's climate was found. This observation is in line with Grace and Norton (1990) who also found no significant positive relationship with climate of the prior summer season relative to the year of ring formation. In order to maximize the temporal extent of each grid-box reconstruction, a nested approach was performed. This procedure iteratively re-calculates the PCR as each shorter series is removed, producing an ensemble of multiple reconstructions for each grid-box, each based on decreasing numbers of predictor chronologies back in time (Cook *et al.*, 2002). The different sections of reconstructions were scaled and spliced to the most recent (maximum predictor) reconstruction in order to correct for systematic changes in the variance structure which can occur due to changing (likely weakening) calibration strength related to the reducing number of predictors back in time.

### 2.7. Reconstruction calibration and verification

For initial tree-ring parameter and detrending tests, the 1901–2006 period was used for an assessment of reconstruction skill with a split (1901–1953) calibration and (1954–2006) verification period followed by a repeat of the exercise with a 'reversed' (1954–2006) calibration and (1901–1953) verification period. Calibration and verification statistics were then computed using an average of the 'forward' and 'reverse' results. The  $r^2$  statistic was calculated for the calibration (CRSQ) and verification (VRSQ) periods, and the coefficient of efficiency (CE) determined for the verification period. The CE statistic is related to the reduction of error (RE) statistic which measures whether a reconstruction provides a better estimate of climatic variability than the mean of the instrumental data in the calibration period. However, CE can be viewed as a true representation of regression  $r^2$  when applied to independent data and is more difficult to pass because the verification period (rather than the calibration period) is used as the reference (Briffa *et al.*, 1988; Cook *et al.*, 1994). Although most studies that include some assessment of reconstruction skill frequently also report RE, this metric was omitted in this study in favour of utilizing the more stringent CE metric. An additional 'early' independent verification period (1872–1900) was used to further assess reconstruction performance using the full (1901–2006) calibration period. For this early (1872–1900) independent period, all gridded JA mean temperature series were extended by scaling the SMT data to each gridded temperature series according to their common period of overlap.

To allow the incorporation of 'older' MXD chronologies not updated since the late 1970s, while simultaneously

also providing an even more stringent verification procedure, the 1901–1976 period was used for calibration and verification for the final reconstruction. For this set of reconstructions, 'forward' (1901–1938 cal./1939–1976 ver.) and 'reverse' (1939–1976 cal./1901–1938 ver.) split-period calibration and verification was performed followed by a final calibration over the full 1901–1976 period. In this case, two independent verification periods (late: 1977–2006 and early: 1872–1900) were used for an additional evaluation of reconstruction skill outside the full 1901–1976 calibration period.

## 3. Results

A summary of PPR reconstruction tests, which demonstrate the effect of varying the minimum number of site chronologies required to perform a reconstruction for each grid-box using calibration and verification statistics, is presented in Figure 2. Apart from the early independent period verification  $r^2$  (VRSQ) results, all other results show that the greatest overall improvement and decrease in the inter-quartile range occurs when the minimum number of chronologies is increased from three to four. Thereafter, any improvements due to further increases in the number of chronologies are more subtle. Oddly, the early (1872–1900) period verification  $r^2$  results show a decrease in the median when increasing the number of chronologies from three to four. There is also a decrease in the upper quartile as the number of chronologies increases to six and decreases further still with seven chronologies. Based on this ensemble of calibration and verification test results, a minimum of four chronologies was selected as a suitable limit to perform PPR. For all further PPR analysis, the search radius was therefore iteratively expanded until a minimum of four chronologies were identified and entered into the PCR procedure.

The spatial representation of a series of tests involving calibration and verification statistics (Figure 3), using various tree-ring parameters and standardization techniques, indicates a sensitivity of results to the characteristics, treatment and type of the input data used. Specifically, the weakest results are obtained when only using RW chronologies with NX detrending and without CID correction, with the vast majority of grids portraying weak calibrated coherence and failing verification CE (VCE).

Limited improvement is observed both in the strength of calibration and verification when signal-free and selected CID-corrected versions of RW chronologies are used (Table 1; Figure 3(b)). The addition of BI data (Figure 3(c)) considerably improves the calibration and verification  $r^2$  results, although in general, the verification and early independent period VCE do not exhibit any improvement. A further marked improvement in all statistics is apparent with the application of only the composite chronologies (Figure 3(d)). Importantly, with a few exceptions, the vast majority of grids pass verification ( $CE > 0$ ), although with weaker results in the west and northwest. Compared with the analysis in Figure 3(d), which only includes the

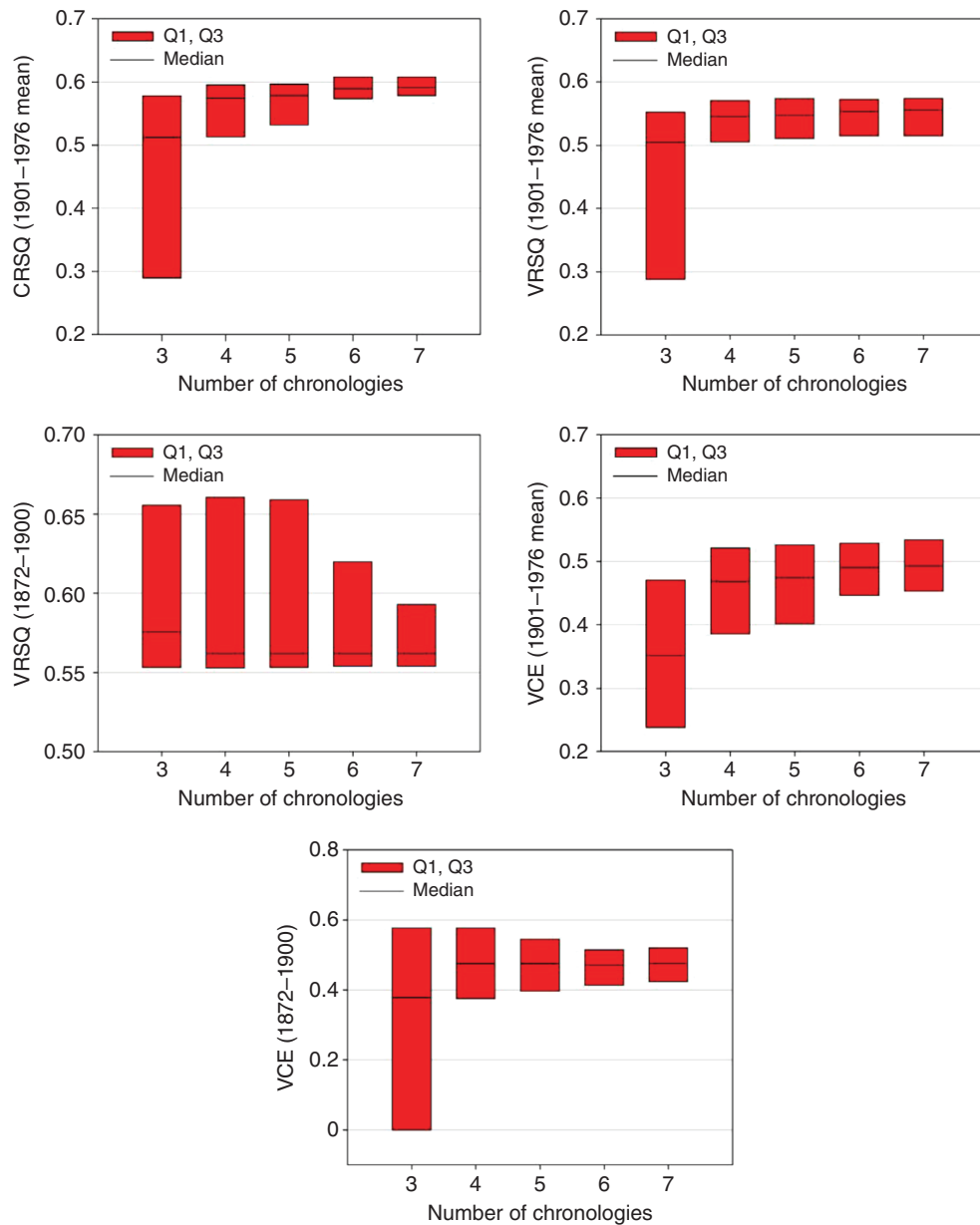


Figure 2. Calibration and verification statistics for an ensemble analysis with varying minimum required number of site chronologies for grid reconstruction. Each panel comprises data from all 76 grid boxes (Q1, Q3 represents the inter-quartile range).

composite chronologies, the inclusion of new MXD data in addition to the composite chronologies (Figure 3(e)) in general yields similar results. However, in the latter version all reconstructions pass the verification tests despite slightly weaker overall verification.

To allow the inclusion of additional MXD data used by Hughes *et al.* (1984), the analysis from Figure 3(e) was repeated with a shorter (1901–1976) calibration and verification period (Figure 4). The calibration and verification  $r^2$  and VCE are broadly similar to their Figure 3(e) counterparts, although notably somewhat weaker for southern and northwest Scotland. In contrast to the results of Figure 3(e), early period VCE results appear stronger in the west and northwest and weaker in the east and south of Scotland. A pattern of weaker late independent period VCE is apparent in the northwest and also in southern Scotland.

The distribution of many Scottish mainland instrumental temperature records is spatially biased to locations in (north-) eastern and southern Scotland, as is also reflected in the composition of the SMT temperature data set (see inset map in Figure 1). For this reason, gridded temperature data in NW Scotland may include a possible bias to the Stornoway station in the Outer Hebrides with more of a maritime influence. To explore spatial variations in reconstruction skill as a function of site chronologies while disregarding differences in the gridded temperature data set, an additional reconstruction of the field was performed. By undertaking the analysis presented in Figure 4 with a single common instrumental temperature series for all grid boxes (i.e. using the Jones and Lister (2004) SMT JA temperature data – see Figure S3), the influence of differences between local gridded temperature series on reconstruction

SPATIAL RECONSTRUCTION OF SCOTTISH SUMMER TEMPERATURES

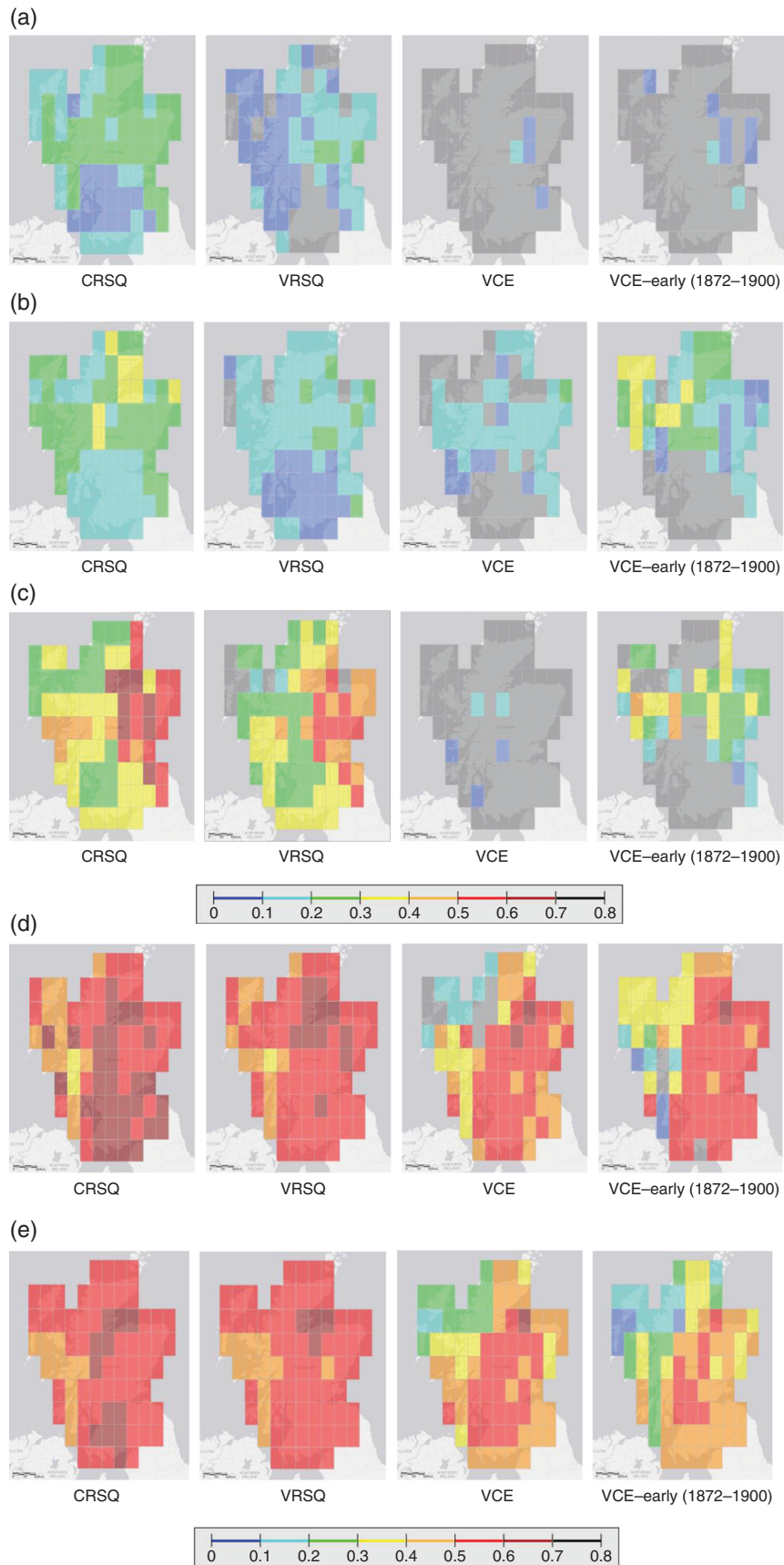


Figure 3. Mean of forward (cal. 1901–1953/ver. 1954–2006) and reverse (cal. 1901–1953/ver. 1954–2006) calibration (CRSQ), verification (VRSQ)  $r^2$  and verification CE (VCE), and early independent verification period CE (VCE 1872–1900) with predictor data including (a) RW (NX, pre-CID); (b) RW (SF, pre/post-CID); (c) RW (SF, pre/post-CID) & BI – separate chronologies; (d) RW (SF, pre/post-CID) + BI – composite chronologies and (e) RW (SF, pre/post-CID) + BI – composite chronologies & separate MXD chronologies.

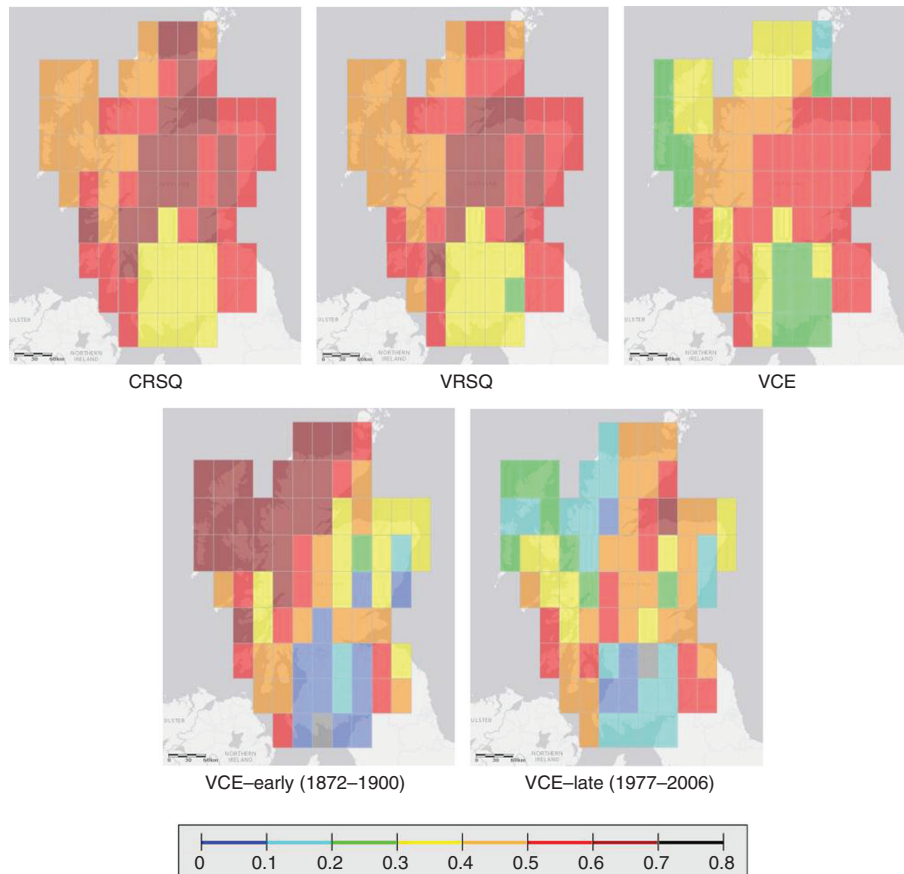


Figure 4. Mean of forward (cal. 1901–1938/ver. 1939–1976) and reverse (cal. 1939–1976/ver. 1901–1938) calibration (CRSQ), verification (VRSQ)  $r^2$  and verification CE (VCE), and early (1872–1900) and late (1977–2006) independent verification period CE. Reconstructions are based on RW (SF, pre/post-CID) + BI – composite chronologies & separate MXD chronologies.

results is removed and so differences arising only from variations in the tree-ring chronologies can be assessed more clearly. Any limitations of using a single temperature series for this analysis should be minimal considering the high degree of agreement of the SMT series with the gridded temperatures ( $r > 0.96$  with the majority of Scottish mainland grid boxes and  $r > 0.9$  with all investigated grid boxes – see Figure S4). In this way, a sense of any limitations of the instrumental temperature data sets, as well as the relative strengths and weaknesses of the tree-ring chronologies, can be gained. Despite some minor differences, these results broadly agree with the patterns identified in Figure 4.

Using the same input chronologies as in Figure 4, the early (1872–1900) and late (1977–2006) VCE displayed in 50 year steps from 1850 back to 1650 express the decreasing spatial coverage and (generally) decreasing strength of the nested reconstructions as the number of chronologies in each nest declines in earlier time periods (Figure 5). While the VCE results for 1850 are largely comparable to those of the most recent nest in Figure 4, by 1800 a group of grids in the south do not pass late independent period VCE. For the reconstruction nests extending back to 1750, weakening of the verification results is apparent, with early independent verification period CE dropping to  $\leq 0$  in a set of

grids in the east and northeast of Scotland. Most of the grid reconstructions in northern and northeast Scotland end between 1700 and 1750, although VCE results for most of the remaining grids do not show any considerable weakening and in fact some show improvement compared to the 1750 nests in certain areas (e.g. eastern Scotland).

Individual grid reconstructions from three example regions are presented in Figure 6. Absolute reconstructed temperatures (Figure 6(a) and (b)) show highest levels in the south, lower values in the northwest and the lowest temperatures in the central-east part of Scotland (see Figure S5 for separate plots of instrumental and reconstructed series for each of the three grid boxes). When expressed as temperature anomalies (Figure 6(d)), different trends and departures can be discerned in the regional patterns of temperature variability over time. In relation to the other two reconstructions, the amplitude of the central-east reconstruction is greater. While the general trends are similar between the three variants, some notable differences are apparent. Temperatures are reconstructed as relatively higher from  $\sim 1730$  until 1900 for the south in relation to reconstructions from the two regions farther north, which also exhibit greater overall similarity. In addition, the late 19th century stands out as a relatively cooler period in the central-eastern Highlands. Although

SPATIAL RECONSTRUCTION OF SCOTTISH SUMMER TEMPERATURES

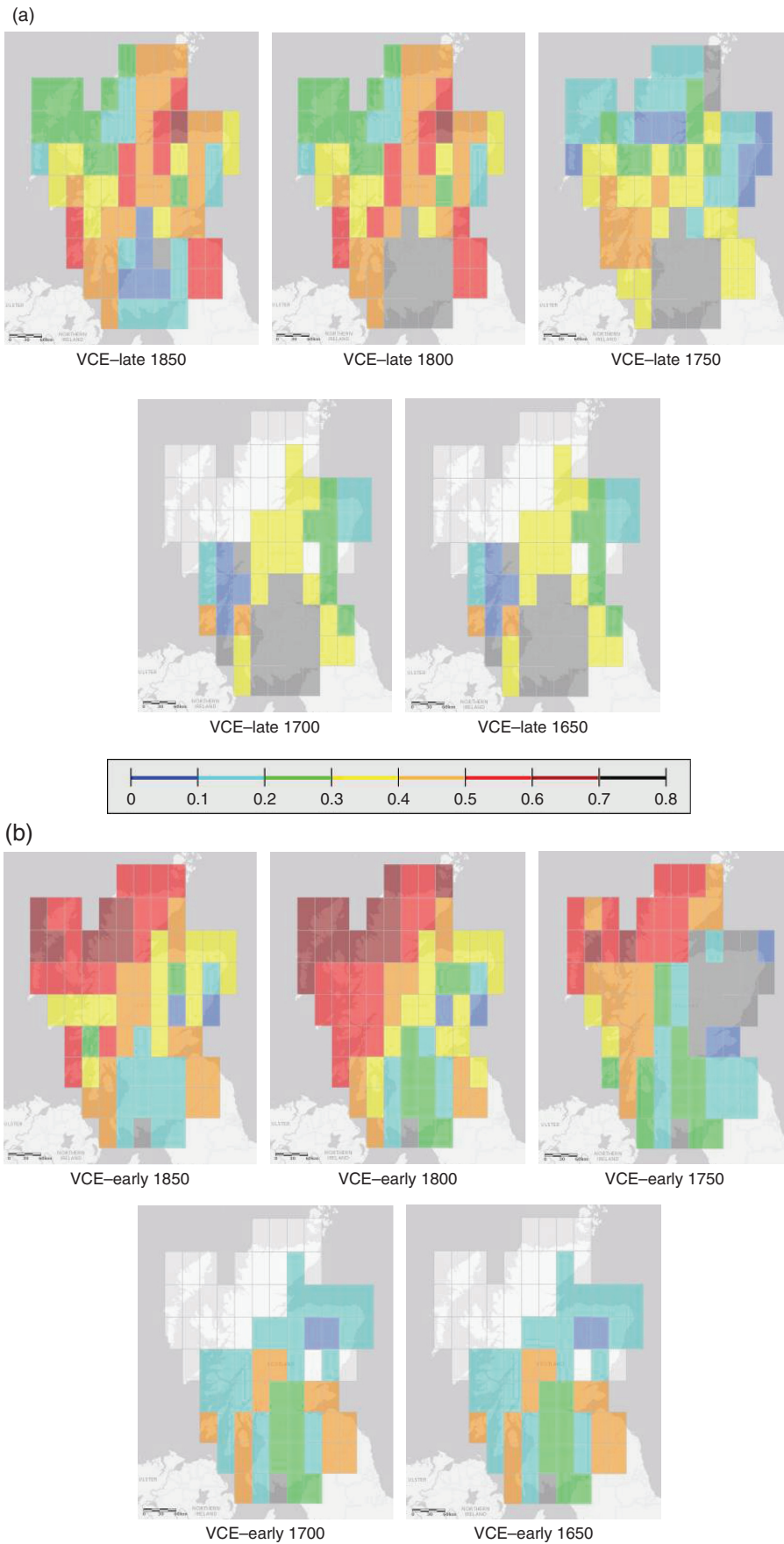


Figure 5. Independent verification CE (VCE) for the (a) late (1977–2006) and (b) early (1872–1900) period with reconstruction nests in 50-year intervals. Reconstructions are based on RW (SF, pre/post-CID) + BI – composite chronologies & separate MXD chronologies (white grids signify no available data for a specific period. Grey grids represent  $VCE \leq 0$ .)

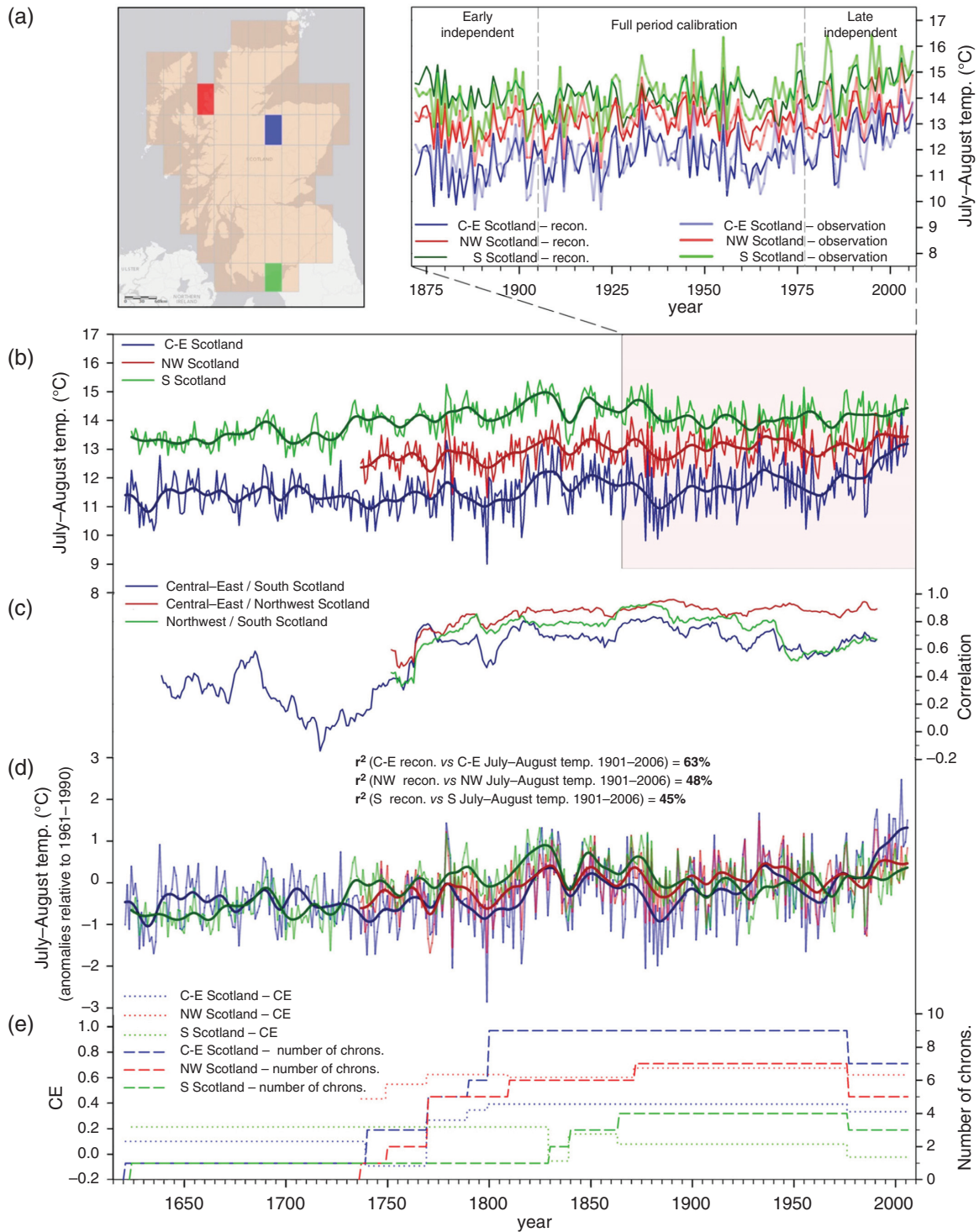


Figure 6. Reconstructions for selected grid boxes from the central-east, northwest and south of Scotland. Reconstructions are displayed as absolute reconstructed July–August temperatures (a) over the 1872–2006\* period together with the respective instrumental temperature for each location, (b) for the full reconstruction length including low-pass filtered (20-year Gaussian filter) versions, (c) with moving 31-year correlation windows for each reconstruction pair, (d) as temperature anomalies relative to the 1961–1990 period including low-pass filtered versions and (e) showing the number of predictor chronologies and CE for the 1872–1900 period [\*Instrumental temperatures before 1901 are represented by Jones and Lister (2004) temperature data scaled to each gridded temperature series over the common period of overlap].

1799 is reconstructed as the coldest year for the JA season in the nearly 400 year reconstruction for central-eastern Scotland, this negative departure is less prominent in the northwest version and virtually absent in the southern reconstruction. Furthermore, some differences in trend are

apparent, particularly in the southern grid reconstruction, around the mid-20th century and also in the early and mid-18th century. These differences may represent an expression of the weaker calibration/verification results of the southern grids (Figures 4 and 5).

Differences in reconstructed late 20th century temperatures are characterized by the greatest temperature increase for the central-east, a less prominent increase for the northwest and an even flatter reconstructed recent period for southern Scotland. Accordingly, correlations between reconstructed and gridded instrumental temperatures for the 1901–2006 period indicate that agreement with observed temperature is strongest for the central-east reconstruction ( $r^2 = 63\%$ ;  $p < 0.001$ ) followed by the northwest ( $r^2 = 48\%$ ;  $p < 0.001$ ) and weaker still for the south of Scotland ( $r^2 = 45\%$ ;  $p < 0.001$ ). Examination of the regression residuals also indicates significant linear trends for the northwest and south Scotland reconstructions (correlation between residuals and time –  $r_{(\text{south})} = 0.35$ ,  $p < 0.001$ ;  $r_{(\text{northwest})} = 0.39$ ,  $p < 0.001$ ;  $r_{(\text{central-east})} = 0.07$ ,  $p = 0.508$ ). Sliding correlations between each reconstruction pair (Figure 6(c)) indicate strong agreement between the central-east and northwest reconstructions for most of their common period. Agreement between the south and central-east reconstructions is generally weaker than between the south and northwest versions, although weaker agreement of the southern reconstruction in relation to the other two versions is evident in the second half of the 20th century. The correlation between the south and central-east reconstructions decreases markedly for much of the period prior to ~1760.

#### 4. Discussion

Ensemble test results have been shown to enable an informed decision about selecting a suitable minimum number of input chronologies while also attempting to retain information about patterns of spatial variability which may otherwise be lost with the integration of information from chronologies over a larger area. The greatest gains are achieved when the minimum number of chronologies used increases from three to four. Increasing the number of chronologies beyond four may still result in some, though limited, improvement (Figure 2). One exception are the weaker VRSQ (1872–1900) results as the number of predictor chronologies increases. This may simply reflect the inclusion of chronologies, which happen to be weaker over this particular period, in a larger number of grid-box reconstructions. For the reconstruction of this particular temperature grid, the selection of four chronologies as the minimum number of predictors is, therefore, a reasonable compromise between preserving regional detail in spatial patterns of variability and developing statistically robust temperature reconstructions.

Clearly, it is not possible to develop reliable reconstructions for the majority of Scotland using only RW data and standard NX detrending (Figure 3(a)). Although the application of more refined methods such as signal-free detrending in combination with CID-based disturbance correction improves results, indicating that disturbance is a contributing factor to the poor results, they still remain relatively weak due to the limited strength of RW as a predictor of

high frequency temperature (Figure 3(b)). The addition of BI chronologies helps to improve the strength of CRSQ and VRSQ (Figure 3(c)) due to the stronger high to intermediate frequency response of BI to temperature. However, BI chronologies alone (as traditionally developed) do not augment the results of the verification tests (i.e. VCE) due to the weaker expression of lower frequency trends related to heartwood/sapwood colour differences (Rydval *et al.*, 2014). The combination of BI and RW data to form composite chronologies substantially improves both calibration and verification results (Figure 3(d)) beyond that achieved using each parameter separately by reducing some of the limitations of each parameter. In the absence of MXD data, this BI/RW composite still provides improved temperature reconstructions for most parts of Scotland, although the addition of MXD chronologies (Figure 3(e)) does improve verification of some grids in the northwest. Thus, the latter option is currently the most appropriate for reconstructing temperature with tree-ring data in Scotland.

Absolute differences in reconstructed temperature from the three selected regions (Figure 6) reflect latitudinal and elevational differences represented in the gridded data. The generally good agreement between the central-east and northwest reconstructions before about 1990 indicates that considerable confidence can be placed in the reconstructions back to the mid-18th century and that any limitation of the northwest reconstruction is restricted to the most recent ~20-year period. However, greater disagreement before ~1750 suggests that the reliability of these earlier reconstructed segments may be questionable and is likely a consequence of lower sample replication and the small number of chronologies in this ‘early’ period. As also indicated by the calibration and verification assessment statistics, the southern reconstruction is the least reliable due to periods of disagreement with the two other reconstructions, weaker agreement with instrumental data and its failure (similarly to the northwest reconstruction) to capture the late 20th century temperature increase as indicated by the linear residual trend.

Although some grid-box reconstructions represent an interpolation of chronology predictors located outside the grid boxes, others (such as the example southern series in Figure 6) are essentially spatial extrapolations with respect to the location of sites used to reconstruct them (Figure 1). Although these extrapolated grid-box reconstructions express some skill, the absence of chronologies from peripheral locations could contribute to reduced calibration and verification strength for those areas.

In addition, because the longer SMT record (extending back to 1866) was developed with instrumental records from southern and eastern parts of mainland Scotland (see inset map in Figure 1), one might argue that the record may not be representative of temperatures in the west or northwest of Scotland and therefore may not be a suitable data set for extending the gridded temperature series before 1901. However, the strong early independent period (1872–1900) VCE results in Figure 4 for the northwest suggest that this record is still of relevance to those areas, which is also supported by strong agreement

between the SMT and gridded data in these locations (see Figure S4). Furthermore, the relatively weak late period VCE results (representing analysis involving the gridded temperature data) suggest that the post-1976 period is the source of the weaker results for the northwest and therefore likely reflects limitations in the tree-ring data. One may also argue that rather than being a limitation of the site chronologies, a possible alternative explanation for weaker results in the northwest may relate to a limitation of the *gridded* instrumental data set itself which may not be representative of the local conditions in this area due to limited spatial and temporal coverage of instrumental records in some (particularly the marginal) areas of Scotland. However, because similar results to those achieved when using the CRU TS3.10 gridded temperature data (Figure 4) were obtained when using only SMT data for each grid (see Figure S3), this again suggests that areas with weaker calibration and verification results likely reflect limitations of the tree-ring chronologies rather than any limitations of the actual instrumental data.

Calibration and verification is strongest around central Scotland and generally weaker in the northwest and particularly the south, which is expressed in Figure 6 by flatter late 20th century reconstructed temperatures for both areas in addition to a relatively warmer 19th century in the south. The weaker reconstructions (particularly in the south) could be attributed to some combination of three primary factors including: (1) differences in site elevation (and perhaps also latitude) (Table 1) that may affect the importance of temperature in limiting growth, (2) limitations of the CID procedure (which would arguably affect the West Highland chronologies more than sites in the Cairngorms as they generally experienced a greater degree of human related disturbance particularly around the Napoleonic Wars at the beginning of the 19th century – Rydval *et al.*, 2016) and (3) differences in the number of chronologies entering PCR analysis.

It is interesting to note that reconstruction strength coincides with elevational (and latitudinal) variations reflected by differences in mean temperature across Scotland (Figure 6(a)), with higher mean temperatures in the northwest and higher still in the south. While it is true that some grid-box series are reconstructed using chronologies from sites that are not in their immediate vicinity, sites in the (north-) west and south are generally located at lower elevations than sites in the central-east area (Figure 1 and Table 1). Therefore, because reconstructions in the northwest and south are primarily developed with chronologies from lower elevation sites, the weaker reconstruction results may partly be related to a potentially weaker temperature signal in lower elevation and / or more southern site chronologies (i.e. farther away from the treeline).

Likewise, differences in the variance of the reconstructions in Figure 6 could also be explained by differences in site elevation/latitude and perhaps related differences in chronology sensitivity to temperature since the southern reconstruction is the least variable ( $\sigma^2_{(1901-2006)} = 0.26$ ) followed by the northwest reconstruction ( $\sigma^2_{(1901-2006)} = 0.32$ ) while in contrast the

central-east reconstruction contains the most variance ( $\sigma^2_{(1901-2006)} = 0.71$ ). This would presumably be due to variations in the ability (of stands at different sites) to capture temperature information. Although the variance of the gridded instrumental data ( $\sigma^2_{(northwest)} = 0.69$ ;  $\sigma^2_{(central-east)} = 1.02$ ;  $\sigma^2_{(south)} = 0.93$  for 1901–2006) also differs and a lower amount of explained variance from the regression (Figure 6(d)) would also lead to a reduction in variance, the differences alone are not sufficient to explain these variations, particularly between the central-east and south reconstructions. However, these factors may largely account for the lower variance of the northwest reconstruction. Although previous research has suggested that differences in site elevation may not have a strong influence on growth response to temperature in Scotland (Grace and Norton, 1990), these conclusions were reached from only a small number of sites in the NW Cairngorms where calibration is strong. Although a detailed examination of such effects is beyond the scope of this study, the importance of such factors should, however, be investigated and re-evaluated in the future using a more extensive network of sites.

A comparison of the southern reconstruction with the other two in Figure 6(d) suggests that the influence of disturbance was either not entirely removed or that other factors affected growth. The limited performance of southern reconstructions can, in part, be accounted for by the versions of RW chronologies used to develop these reconstructions. Although a general improvement was observed by using CID-corrected chronologies (Rydval *et al.*, 2016), the method may not have accurately identified all disturbance events. More importantly, some disturbance trends may have remained because pre-correction chronologies were used for reconstruction (see Table 1) when post-correction versions showed no improvement. The Glen Falloch chronology, which is the longest of the southern sites, is one example where the pre-correction version was used. There is therefore a need to focus on updating and extending chronologies at other southern sites such as Glen Orchy and Coille Coire Chuilc, where additional suitable older stands exist (or which could be extended with historical material), in order to develop ‘cleaner’ reconstructions for this region.

While not specifically assessed as part of the work presented herein, the importance of additional factors such as high-wind stress and high rates of precipitation leading to excessive soil moisture in parts of the Highlands should not be underestimated and may require additional examination in the future. The most practical approach for improving reconstructions in areas with currently weaker results or limited reconstruction length would involve the development of additional chronologies and increasing early period replication in chronologies containing relatively few older tree series. New sites from more marginal parts of the network could also be sampled (where living stands exist) or existing chronologies extended using subfossil or historical material where possible.

As suitable subfossil sites in the Highlands are rare, the fact that the majority of subfossil samples have been

collected from lochs (lakes) located in the central-east (north Cairngorms) region and used to develop a continuous ~800 year chronology is important in relation to the findings of this study. The strong calibration results indicate that it is among the most suitable areas in Scotland to develop an extended reconstruction. Substantial subfossil material has also been sampled from Glen Affric which should enable a significant extension of this record. However, severe disturbance effects at this location, which may not have been completely removed using CID (Rydval *et al.*, 2016), are still an issue which would need to be addressed in the future. Temporal extension of chronologies from both these regions may also be possible using samples from historical structures. A further effective option to improve the quality of reconstructions would involve re-processing existing samples to develop either new MXD chronologies or developing additional BI chronologies in order to increase the total number of sites for which composite BI/RW chronologies could be produced.

On the whole, the analysis presented herein highlights the importance of developing an awareness and appreciation of tree growth response within the interplay of often confounding climatic, ecological and anthropogenic factors in order to appropriately assess the suitability of tree-ring data for climate reconstruction. Such intricacies have often been overlooked by dendroclimatologists in the past.

## 5. Conclusion

This study utilized an extensive Scottish pine tree-ring network to derive spatial field information by adopting a reconstruction approach specifically intended to preserve sub-regional variations and assess the temperature reconstruction potential of this network. The reconstruction of temperature grids using only conventionally detrended RW data produced weakly calibrated and poorly verified models. Calibration and verification results generally improved after CID disturbance correction and signal-free detrending (Melvin and Briffa, 2008), and with the addition of BI chronologies. Further improvement in reconstruction ‘quality’ was observed by using composite chronologies and by including MXD data.

Weaker calibration results in the northwest likely resulted from limitations in the currently available tree-ring data rather than the gridded temperatures. Limited improvement of some grid reconstructions can be partly attributed to imperfect disturbance detection in CID-corrected chronologies and the use of pre-correction RW chronologies in some instances. However, the CID approach generally improved temperature reconstruction results. Additional factors probably also contributed to weaker results in some areas and so the relationships between tree growth, climatic and non-climatic factors should be investigated further.

Further improvement of reconstruction length and robustness can be achieved by sampling new sites,

developing more BI and MXD chronologies from existing samples, and by including additional samples from longer lived trees and subfossil samples (where material exists). Importantly, the strongest calibration/verification and overall reconstruction results were developed from sites in the Cairngorms (central-east sector). This is encouraging as the majority of subfossil material comes from this region and has been used to develop an extended temperature reconstruction for Scotland (Rydval, 2015). More generally, this work emphasizes the importance of appreciating the interaction of climatic and non-climatic factors when reconstructing climate.

## Acknowledgements

We wish to thank The Carnegie Trust for the Universities of Scotland for providing funding for Miloš Rydval's PhD. The Scottish pine network expansion has been an ongoing task since 2006 and funding must be acknowledged to the following projects: EU project ‘Millennium’ (017008-2), Leverhulme Trust project ‘RELiC: Reconstructing 8000 years of Environmental and Landscape change in the Cairngorms (F/00 268/BG)’ and the NERC project ‘SCOT2K: Reconstructing 2000 years of Scottish climate from tree rings (NE/K003097/1)’. We also thank Rider University for a faculty research fellowship that supported Daniel Druckenbrod, and Paul J. Krusic for compiling and making available a PC version of the point-by-point PCR software. Lamont-Doherty Earth Observatory contribution No. 8032.

## Supporting Information

The following supporting information is available as part of the online article:

**Figure S1.** Pre- and post-CID chronologies for three Scottish regions and their comparison with the SMT July–August mean temperature series.

**Figure S2.** Coherency analysis of RW and BI chronologies from central Scotland with SMT July–August temperature data.

**Figure S3.** Calibration and verification results using the SMT mean July–August temperature series as the reconstruction target for all grids.

**Figure S4.** Spatial correlation plot of SMT July–August mean temperature series with 0.5° CRU TS3.10 mean temperature grid boxes.

**Figure S5.** Local CRU TS3.10 mean July–August instrumental and reconstructed temperatures for grid boxes in three selected locations around Scotland.

## References

- Ahmed M, Anchukaitis KJ, Asrat A, Borgeonkar H, Braida M, Buckley BM, Büntgen U, Chase BM, Christie DA, Cook ER, Curran MAJ, Diaz HF, Esper J, Fan ZX, Gaire NP, Ge Q, Gergis J, González-Rouco JF, Goosse H, Grab SW, Graham N, Graham R, Grosjean M, Hanhijärvi ST, Kaufman DS, Kiefer T, Kimura K, Korhola AA, Krusic PJ, Lara A, Lézine AM, Ljungqvist FC, Lorrey AM, Luterbacher J,

- Masson-Delmotte V, McCarroll D, McConnell JR, McKay NP, Morales MS, Moy AD, Mulvaney R, Mundo IA, Nakatsuka T, Nash DJ, Neukom R, Nicholson SE, Oerter H, Palmer JG, Phipps SJ, Prieto MR, Rivera A, Sano M, Severi M, Shanahan TM, Shao X, Shi F, Sigl M, Smerdon JE, Solomina ON, Steig EJ, Stenni B, Thamban M, Trouet V, Turney CS, Umer M, Van Ommen T, Verschuren D, Viau AE, Villalba R, Vinther BM, von Gunten L, Wagner S, Wahl ER, Wanner H, Werner JP, White JW, Yasue K, Zorita E. 2013. Continental-scale temperature variability during the past two millennia. *Nat. Geosci.* **6**(5): 339–346.
- Barnett TP, Preisendorfer R. 1987. Origins and levels of monthly and seasonal forecast skill for United States surface air temperatures determined by canonical correlation analysis. *Mon. Weather Rev.* **115**(9): 1825–1850.
- Briffa KR, Jones PD, Wigley TML, Pilcher JR, Baillie MGL. 1986. Climate reconstruction from tree rings: part 2, spatial reconstruction of summer mean sea-level pressure patterns over Great Britain. *J. Climatol.* **6**(1): 1–15.
- Briffa KR, Jones PD, Pilcher JR, Hughes MK. 1988. Reconstructing summer temperatures in northern Fennoscandia back to AD 1700 using tree-ring data from Scots pine. *Arct. Alp. Res.* **20**(4): 385–394.
- Briffa KR, Melvin TM, Osborn TJ, Hantemirov RM, Kirilyanov AV, Mazepa VS, Shiyatov SG, Esper J. 2013. Reassessing the evidence for tree-growth and inferred temperature change during the Common Era in Yamalia, northwest Siberia. *Quat. Sci. Rev.* **72**(8): 83–107.
- Cook ER, Holmes RL. 1986. Users manual for program ARSTAN. In *Tree-Ring Chronologies of Western North America*, Holmes RL, Adams RK, Fritts HC (eds). University of Arizona: Tucson, AZ, 50–65.
- Cook ER, Peters K. 1997. Calculating unbiased tree-ring indices for the study of climatic and environmental change. *Holocene* **7**(3): 361–370.
- Cook ER, Briffa KR, Jones PD. 1994. Spatial regression methods in dendroclimatology: a review and comparison of two techniques. *Int. J. Climatol.* **14**(4): 379–402.
- Cook ER, Meko DM, Stahle DW, Cleaveland MK. 1999. Drought reconstructions for the continental United States. *J. Clim.* **12**(4): 1145–1162.
- Cook ER, D'Arrigo RD, Mann ME. 2002. A well-verified, multiproxy reconstruction of the winter North Atlantic Oscillation Index since ad 1400. *J. Clim.* **15**(13): 1754–1764.
- Cook ER, Esper J, D'Arrigo RD. 2004. Extra-tropical Northern Hemisphere land temperature variability over the past 1000 years. *Quat. Sci. Rev.* **23**(20): 2063–2074.
- Cook ER, Anchukaitis KJ, Buckley BM, D'Arrigo RD, Jacoby GC, Wright WE. 2010. Asian monsoon failure and megadrought during the last millennium. *Science* **328**(5977): 486–489.
- Cook ER, Krusic PJ, Anchukaitis KJ, Buckley BM, Nakatsuka T, Sano M. 2013. Tree-ring reconstructed summer temperature anomalies for temperate East Asia since 800 CE. *Clim. Dyn.* **41**(11–12): 2957–2972.
- Cook ER, Seager R, Kushnir Y, Briffa KR, Büntgen U, Frank D, Krusic PJ, Tegel W, van der Schrier G, Andreu-Hayles L, Baillie M, Baitinger C, Bleicher N, Bonde N, Brown D, Carrer M, Cooper R, Čufar K, Dittmar C, Esper J, Griggs C, Gunnarson B, Günther B, Gutierrez E, Haneca K, Helama S, Herzog F, Heussner K-U, Hofmann J, Janda P, Kotic R, Köse N, Kyncl T, Levanić T, Linderholm H, Manning S, Melvin TM, Miles D, Neuwirth B, Nicolussi K, Nola P, Panayotov M, Popa I, Rothe A, Seftigen K, Seim A, Svarva H, Svoboda M, Thun T, Timonen M, Touchan R, Trotsiuk V, Trouet V, Walder F, Ważny T, Wilson R, Zang C. 2015. Old World megadroughts and pluvials during the Common Era. *Sci. Adv.* **1**(10): e1500561, doi: 10.1126/sciadv.1500561.
- Cook BI, Anchukaitis KJ, Touchan R, Meko DM, Cook ER. 2016. Spatiotemporal drought variability in the Mediterranean over the last 900 years. *J. Geophys. Res.* **121**(5): 2060–2074.
- Crone A, Mills CM. 2002. Seeing the wood and the trees: dendrochronological studies in Scotland. *Antiquity* **76**(293): 788–794.
- Dannenberg MP, Wise EK. 2013. Performance of climate field reconstruction methods over multiple seasons and climate variables. *J. Geophys. Res.* **118**(17): 9595–9610.
- Dawson AGD. 2009. *So Foul and Fair a Day: A History of Scotland's Weather and Climate*. Birlinn: Edinburgh, 230.
- Druckenbrod DL. 2005. Dendroecological reconstructions of forest disturbance history using time-series analysis with intervention detection. *Can. J. For. Res.* **35**(4): 868–876.
- Druckenbrod DL, Pederson N, Rentch J, Cook ER. 2013. A comparison of times series approaches for dendroecological reconstructions of past canopy disturbance events. *For. Ecol. Manage.* **302**: 23–33.
- Esper J, Frank DC, Wilson RJ, Briffa KR. 2005. Effect of scaling and regression on reconstructed temperature amplitude for the past millennium. *Geophys. Res. Lett.* **32**(7): L07711, doi: 10.1029/2004GL021236.
- Fang K, Gou X, Chen F, Cook E, Li J, Buckley B, D'Arrigo R. 2011. Large-scale precipitation variability over northwest China inferred from tree rings. *J. Clim.* **24**(13): 3457–3468.
- Folland CK, Knight J, Linderholm HW, Fereday D, Ineson S, Hurrell JW. 2009. The summer North Atlantic Oscillation: past, present, and future. *J. Clim.* **22**(5): 1082–1103.
- Forestry Commission. 2011. *National Forest Inventory Woodland Area Statistics: Scotland*. Forestry Commission: Edinburgh, 17.
- Fritts HC. 1976. *Tree Rings and Climate*. Academic Press: London, 567 pp.
- Gallardo C, Gil V, Hagele E, Tejada C, de Castro M. 2013. Assessment of climate change in Europe from an ensemble of regional climate models by the use of Köppen–Trewartha classification. *Int. J. Climatol.* **33**(9): 2157–2166.
- Grace J, Norton DA. 1990. Climate and growth of *Pinus sylvestris* at its upper altitudinal limit in Scotland: evidence from tree growth-rings. *J. Ecol.* **78**(3): 601–610.
- Guay R, Gagnon R, Morin H. 1992. A new automatic and interactive tree ring measurement system based on a line scan camera. *Forest. Chron.* **68**(1): 138–141.
- Guiot J. 1985. The extrapolation of recent climatological series with spectral canonical regression. *J. Climatol.* **5**(3): 325–335.
- Guiot J. 2012. A robust spatial reconstruction of April to September temperature in Europe: comparisons between the medieval period and the recent warming with a focus on extreme values. *Glob. Planet. Change* **84**: 14–22.
- Gunnarson BE, Josefsson T, Linderholm HW, Östlund L. 2012. Legacies of pre-industrial land use can bias modern tree-ring climate calibrations. *Clim. Res.* **53**(1): 63–76.
- Harris I, Jones PD, Osborn TJ, Lister DH. 2014. Updated high-resolution grids of monthly climatic observations – the CRU TS3.10 Dataset. *Int. J. Climatol.* **34**(3): 623–642.
- Holmes RL. 1983. Computer-assisted quality control in tree-ring dating and measurement. *Tree-Ring Bull.* **43**: 69–75.
- Hughes MK, Schweingruber FH, Cartwright D, Kelly PM. 1984. July–August temperature at Edinburgh between 1721 and 1975 from tree-ring density and width data. *Nature* **308**: 341–344.
- Hurrell JW. 1995. Decadal trends in the North Atlantic Oscillation: regional temperatures and precipitation. *Science* **269**(5224): 676–679.
- Hurrell JW, Deser C. 2010. North Atlantic climate variability: the role of the North Atlantic Oscillation. *J. Marine Syst.* **79**(3): 231–244.
- Hurrell JW, van Loon H. 1997. Decadal variations in climate associated with the North Atlantic Oscillation. *Clim. Change* **36**(3–4): 301–326.
- Hurrell JW, Kushnir Y, Ottersen G, Visbeck M. 2003. An overview of the North Atlantic oscillation. In *The North Atlantic Oscillation: Climatic Significance and Environmental Impact*. Geophysical Monograph Series 134, Hurrell JW, Kushnir Y, Ottersen G, Visbeck M (eds). American Geophysical Union: Washington, DC, 1–35.
- IPCC. 2014. Climate change 2014: synthesis report. In *Contribution of Working Groups I, II and III to the Fifth Assessment Report of the Intergovernmental Panel on Climate Change*, Pachauri RK, Meyer LA (eds). IPCC: Geneva, Switzerland, 151 pp.
- ITRDB – International Tree-Ring Data Bank. 2014. *National Climatic Data Center* [Online]. <http://www.ncdc.noaa.gov/data-access/paleoclimatology-data/datasets/tree-ring> (accessed 20 October 2014).
- Jones PD, Lister D. 2004. The development of monthly temperature series for Scotland and Northern Ireland. *Int. J. Climatol.* **24**(5): 569–590.
- Jones PD, Briffa KR, Osborn TJ, Lough JM, van Ommen TD, Vinther BM, Luterbacher J, Wahl ER, Zwiwerski FW, Mann ME, Schmidt GA, Ammann CM, Buckley BM, Cobb KM, Esper J, Goosse H, Graham N, Jansen E, Kiefer T, Kull C, Küttel M, Mosley-Thompson E, Overpeck JT, Riedwyl N, Schulz M, Tudhope AW, Villalba R, Wanner H, Wolff E, Xoplaki E. 2009. High-resolution palaeoclimatology of the last millennium: a review of current status and future prospects. *Holocene* **19**(1): 3–49.
- Josefsson T, Gunnarson B, Liedgren L, Bergman I, Östlund L. 2010. Historical human influence on forest composition and structure in boreal Fennoscandia. *Can. J. For. Res.* **40**(5): 872–884.
- Kinloch BB, Westfall RD, Forrest GI. 1986. Caledonian Scots pine: origins and genetic structure. *New Phytol.* **104**(4): 703–729.
- Körner C. 1998. A re-assessment of high elevation treeline positions and their explanation. *Oecologia* **115**(4): 445–459.

- Larsson L. 2014. *CooRecorder and Cdendro programs of the CooRecorder/Cdendro package version 7.7* [Online]. <http://www.cybis.se/forfun/dendro> (accessed 3 January 2014).
- Linderholm HW, Folland CK, Walther A. 2009. A multicentury perspective on the summer North Atlantic Oscillation (SNAO) and drought in the eastern Atlantic Region. *J. Quat. Sci.* **24**(5): 415–425.
- Luterbacher J, Dietrich D, Xoplaki E, Grosjean M, Wanner H. 2004. European seasonal and annual temperature variability, trends, and extremes since 1500. *Science* **303**(5663): 1499–1503.
- Mather AS. 2004. Forest transition theory and the reforestation of Scotland. *Scot. Geogr. Mag.* **120**(1–2): 83–98.
- Melvin TM, Briffa KR. 2008. A “signal-free” approach to dendroclimatic standardisation. *Dendrochronologia* **26**(2): 71–86.
- Met Office. 2015. *UK Regional Climates* [Online]. <http://www.metoffice.gov.uk/climate/uk/regional-climates> (accessed 10 April 2015).
- Moir AK. 2008. *The Dendroclimatology of Modern and Neolithic Scots pine (Pinus sylvestris L.) in the peatlands of northern Scotland*. PhD thesis, Brunel University, London, UK.
- Mosteller F, Tukey JW. 1977. *Data Analysis and Regression*. Addison-Wesley: Reading, MA.
- Osborn TJ, Briffa KR. 2000. Revisiting timescale-dependent reconstruction of climate from tree-ring chronologies. *Dendrochronologia* **18**: 9–25.
- Osborn TJ, Briffa KR, Jones PD. 1997. Adjusting variance for sample size in tree-ring chronologies and other regional mean timeseries. *Dendrochronologia* **15**: 89–99.
- Quine CP, White IMS. 1993. *Revised Windiness Scores for the Windthrow Hazard Classification: The Revised Scoring Method*. Forestry Commission Research Information Note No. 230, Forestry Commission, Edinburgh, 6.
- Rydval M. 2015. *Dendroclimatic Reconstruction of Late Holocene Summer Temperatures in the Scottish Highlands*. PhD thesis, University of St Andrews, St Andrews, UK.
- Rydval M, Larsson LÅ, McGlynn L, Gunnarson BE, Loader NJ, Young GH, Wilson R. 2014. Blue intensity for dendroclimatology: should we have the blues? Experiments from Scotland. *Dendrochronologia* **32**(3): 191–204.
- Rydval M, Druckenbrod D, Anchukaitis KJ, Wilson R. 2016. Detection and removal of disturbance trends in tree-ring series for dendroclimatology. *Can. J. For. Res.* **46**(3): 387–401.
- Schlesinger ME, Ramankutty N. 1994. An oscillation in the global climate system of period 65–70 years. *Nature* **367**(6465): 723–726.
- Schneider T. 2001. Analysis of incomplete climate data: estimation of mean values and covariance matrices and imputation of missing values. *J. Clim.* **14**(5): 853–871.
- Schweingruber FH. 1988. *Tree Rings-Basics and Applications of Dendrochronology*. Reidel: Dordrecht, Netherlands, 276 pp.
- Schweingruber FH, Fritts HC, Bräker OU, Drew LG, Schär E. 1978. The X-ray technique as applied to dendroclimatology. *Tree-Ring Bull.* **38**: 61–91.
- Seftigen K, Björklund J, Cook ER, Linderholm HW. 2014. A tree-ring field reconstruction of Fennoscandian summer hydroclimate variability for the last millennium. *Clim. Dynam.* **44**(11–12): 3141–3154.
- Shi F, Yang B, Von Gunten L. 2012. Preliminary multiproxy surface air temperature field reconstruction for China over the past millennium. *Sci. China Earth Sci.* **55**(12): 2058–2067.
- Smout TC, MacDonald AR, Watson F. 2005. *A History of the Native Woodlands of Scotland, 1500–1920*. Edinburgh University Press: Edinburgh, 434.
- Štěpánek P. 2008. *AnClim – Software for Time Series Analysis*. Department of Geography, Faculty of Natural Sciences, Masaryk University: Brno, Czech Republic.
- Steven HM, Carlisle A. 1959. *The Native Pinewoods of Scotland*. Oliver and Boyd: Edinburgh, 368.
- Stokes MA, Smiley TL. 1968. *An Introduction to Tree-Ring Dating*. University of Chicago Press: Chicago, IL, 95 pp.
- Thompson DW, Wallace JM. 1998. The Arctic Oscillation signature in the wintertime geopotential height and temperature fields. *Geophys. Res. Lett.* **25**(9): 1297–1300.
- Touchan R, Anchukaitis KJ, Meko DM, Sabir M, Attalah S, Aloui A. 2011. Spatiotemporal drought variability in northwestern Africa over the last nine centuries. *Clim. Dynam.* **37**(1–2): 237–252.
- Trigo RM, Osborn TJ, Corte-Real JM. 2002. The North Atlantic Oscillation influence on Europe: climate impacts and associated physical mechanisms. *Clim. Res.* **20**(1): 9–17.
- Warren WG. 1980. On removing the growth trend from dendrochronological data. *Tree-Ring Bull.* **40**: 35–44.
- Wilson R, Luckman B. 2003. Dendroclimatic reconstruction of maximum summer temperatures from upper treeline sites in Interior British Columbia, Canada. *Holocene* **13**(6): 851–861.
- Wilson R, Loader NJ, Rydval M, Patton H, Frith A, Mills CM, Crone A, Edwards C, Larsson L, Gunnarson BE. 2012. Reconstructing Holocene climate from tree rings: the potential for a long chronology from the Scottish Highlands. *Holocene* **22**(1): 3–11.
- Yang F, Wang N, Shi F, Ljungqvist FC, Wang S, Fan Z, Lu J. 2013. Multi-proxy temperature reconstruction from the West Qinling Mountains, China, for the past 500 years. *PLoS One* **8**(2): e57638, doi: 10.1371/journal.pone.0057638.
- Zhang Z, Mann ME, Cook ER. 2004. Alternative methods of proxy-based climate field reconstruction: application to summer drought over the conterminous United States back to AD 1700 from tree-ring data. *Holocene* **14**(4): 502–516.